

*Comparison of different WSGG correlations in the computation of thermal radiation in a 2D axisymmetric turbulent non-premixed methane–air flame*

**Felipe Roman Centeno, Fabiano Cassol, Horácio A. Vielmo, Francis Henrique Ramos França & Cristiano Vitorino da Silva**

**Journal of the Brazilian Society of Mechanical Sciences and Engineering**

ISSN 1678-5878  
Volume 35  
Number 4

J Braz. Soc. Mech. Sci. Eng. (2013)  
35:419-430  
DOI 10.1007/s40430-013-0040-z



**Your article is protected by copyright and all rights are held exclusively by The Brazilian Society of Mechanical Sciences and Engineering. This e-offprint is for personal use only and shall not be self-archived in electronic repositories. If you wish to self-archive your article, please use the accepted manuscript version for posting on your own website. You may further deposit the accepted manuscript version in any repository, provided it is only made publicly available 12 months after official publication or later and provided acknowledgement is given to the original source of publication and a link is inserted to the published article on Springer's website. The link must be accompanied by the following text: "The final publication is available at [link.springer.com](http://link.springer.com)".**

# Comparison of different WSGG correlations in the computation of thermal radiation in a 2D axisymmetric turbulent non-premixed methane–air flame

Felipe Roman Centeno · Fabiano Cassol ·  
Horácio A. Vielmo · Francis Henrique Ramos França ·  
Cristiano Vitorino da Silva

Received: 25 March 2013 / Accepted: 29 May 2013 / Published online: 19 June 2013  
© The Brazilian Society of Mechanical Sciences and Engineering 2013

**Abstract** This study makes an analysis of the radiation heat transfer in a turbulent non-premixed methane–air cylindrical combustion chamber. The highly complex dependence of the radiative properties with the wavenumber spectrum is modeled with the weighted-sum-of-gray-gas (WSGG), making use of the classical correlations of Smith et al. (J Heat Transfer 104:602–608, 1982) and of the more recently in obtained correlations of Dorigon et al. (IJHMT 64:863–873, 2013), based on HITEMP2010. The reaction rates were considered as the minimum values between the Arrhenius and Eddy Break-Up rates. A two-step global reaction mechanism was used, and turbulence modeling was considered via standard  $k$ – $\epsilon$  model. The source terms of the energy equation consisted of the energy involved in the reaction rates and radiation exchanges. The discrete ordinates method (DOM) was employed to solve

the radiative transfer equation (RTE). The results show that the temperature, the radiative heat source, and the wall heat flux can be importantly affected by the WSGG correlations, while their influence on the species concentrations tends to be negligible. Numerical results considering the WSGG model with the new correlations were closer to experimental data presented in the literature.

**Keywords** Radiation heat transfer · WSGG model · Combustion · Turbulent non-premixed flames

## Symbols

$a_j(T)$	Emission weighted factor (WSGG), dimensionless
$b_j$	Polynomial coefficients of the WSGG model, units can vary
$c$	Each reaction on mechanism, dimensionless
$c_{p,\alpha}$	Specific heat, J/(kg K)
$C_{1,\epsilon}, C_{2,\epsilon}$	Constants of the turbulence model, dimensionless
$C_\mu$	Constant of the turbulence model, dimensionless
CH <sub>4</sub>	Methane
CO	Carbon monoxide
CO <sub>2</sub>	Carbon dioxide
$f_{\text{rad}}$	Radiant fraction, dimensionless
$h$	Specific enthalpy, J/kg
$h_\alpha^0$	Formation enthalpy of species $\alpha$ , J/kg
H <sub>2</sub> O	Water vapor
$I$	Total radiative intensity, W/m <sup>2</sup>
$I_\eta$	Spectral radiative intensity, W/(m <sup>2</sup> m <sup>-1</sup> )
$K$	Turbulent kinetic energy, m <sup>2</sup> /s <sup>2</sup>
$k_j$	Absorption coefficient for the $j$ -th gray gas for WSGG model, m <sup>-1</sup>

Technical Editor: Luis Fernando Figueira da Silva.

F. R. Centeno · F. Cassol · H. A. Vielmo · F. H. R. França (✉)  
Department of Mechanical Engineering,  
Federal University of Rio Grande do Sul, UFRGS,  
Sarmiento Leite Street, no. 425,  
Porto Alegre, RS 90050-170, Brazil  
e-mail: frfranca@mecanica.ufrgs.br

F. R. Centeno  
e-mail: frcenteno@mecanica.ufrgs.br

F. Cassol  
e-mail: fabiano.cassol@ufrgs.br

H. A. Vielmo  
e-mail: vielmoh@mecanica.ufrgs.br

C. V. da Silva  
Universidade Regional Integrada do Alto Uruguai e das Missões,  
URI, Sete de Setembro Avenue, no. 1621,  
Erechim, RS 99700-000, Brazil  
e-mail: cristiano@uricer.edu.br

$k_{p,j}$	Pressure absorption coefficient for the $j$ -th gray gas for WSGG model, $\text{m}^{-1} \text{atm}^{-1}$
$\bar{M}\bar{M}_\alpha$	Molar mass, $\text{kg}/\text{kmol}$
$\mathbf{n}$	Vector normal to the surface element, dimensionless
$N_G$	Number of gray gases (WSGG), dimensionless
$\text{N}_2$	Nitrogen
$\text{O}_2$	Oxygen
$p$	Pressure, Pa
$p_{\text{H}_2\text{O}}/p_{\text{CO}_2}$	Ratio of $\text{H}_2\text{O}$ and $\text{CO}_2$ partial pressures, dimensionless
$p^*$	Modified pressure, Pa
$Pr_b, Sc_t$	Turbulent Prandtl and Schmidt numbers, dimensionless
$\mathbf{q}_r$	Radiative heat flux, $\text{W}/\text{m}^2$
$r$	Radial coordinate, m
$\bar{R}$	Universal gas constant, $\text{J}/(\text{kmol K})$
$R_\alpha$	Volumetric rate of formation or destruction of $\alpha$ , $\text{kg}/(\text{m}^3 \text{s})$
$s$	Distance traveled by the radiation intensity, m
$\mathbf{s}$	Vector in the direction of the radiation intensity, dimensionless
$S_{\text{rad}}$	Radiative heat source, $\text{W}/\text{m}^3$
$S^\phi$	Source term for $\phi$ , $\text{W}/\text{m}^3$
$T$	Temperature, K
$u$	Axial velocity, m/s
$v$	Radial velocity, m/s
$w$	Angular velocity, m/s
$y_\alpha$	Mass fraction, $\text{kg}_\alpha/\text{kg}_{\text{mix}}$
$z$	Axial coordinate, m

**Greek symbols**

$\varepsilon$	Dissipation rate of $k$ , $\text{m}^2/\text{s}^3$
$\varepsilon_w$	Wall emissivity, dimensionless
$\phi$	Generic variable, units can vary
$\varphi$	Angular coordinate, rad
$\Gamma_\phi$	Diffusive coefficient for $\phi$ , $\text{N s}/\text{m}^2$
$\kappa_\eta$	Spectral absorption coefficient, $\text{m}^{-1}$
$\mu$	Viscosity, $\text{N s}/\text{m}^2$
$\mu_t$	Turbulent viscosity, $\text{N s}/\text{m}^2$
$\mu, \varsigma, \xi$	Discrete ordinates method directions
$\rho$	Density, $\text{kg}/\text{m}^3$
$\sigma_k, \sigma_\varepsilon$	Prandtl numbers for $k$ and $\varepsilon$ , dimensionless
$\Omega$	Solid angle, sr

**Subscripts**

$b$	Blackbody
Dorigon	WSGG model coefficients from Dorigon et al. [6]
$j$	Each gray gas of the WSGG model
rad	Radiation
ref	Reference

Smith	WSGG model coefficients from Smith et al. [25]
$w$	Wall
$\alpha$	Each chemical species
$\eta$	Wavenumber, $\text{m}^{-1}$

**1 Introduction**

In non-premixed flames the fuel and oxidant are initially separated, so the combustion is controlled by diffusion and turbulence. Since combustion problems involve a number of coupled phenomena, such as fluid flow, heat transfer and chemical kinetics of gaseous species and soot, an accurate prediction of the thermal radiation heat transfer in participating medium, which can be the dominant heat transfer mode in some combustion processes, is necessary to achieve accurate solutions. Heat transfer directly affects the temperature field, and chemical kinetics can be strongly dependent on temperature; in this way, accurate description of radiative heat transfer is crucial for simulations of combustion systems. On the other hand, its modeling is a difficult task due to the highly complex dependence of the absorption coefficient with the wavenumber, which is typically characterized by hundreds of thousands of spectral lines. Thus, the solution of the radiative heat transfer equation (RTE) is very expensive or even impossible without a model to solve the spectral problem. As a simplification, the RTE is frequently solved with the gray gas (GG) model, where the dependence of the absorption coefficient over the wavenumber is neglected. In order to provide better results, spectral models are commonly used. Among the spectral dependent models, the weighted-sum-of-gray-gases (WSGG) [11] is a method that is still widely used nowadays, especially in global simulation of combustion processes in which the RTE is solved together with fluid flow, chemical kinetics and energy equation. In the WSGG model, the entire spectrum is represented by a few bands having uniform absorption coefficients, each band corresponding to a gray gas. The weighting coefficients account for the contribution of each gray gas, representing the fractions of the blackbody energy in the spectrum region where the gray gases are located. In practice, those coefficients are obtained from fitting total emittances computed from experimental-gas-data, such as those presented in Smith et al. [24] and Smith et al. [25]. In a recent study, Demarco et al. [5] assessed several radiative models, such as narrow band, wide band, GG and global models as the WSGG and the spectral-line-based WSGG (SLW), and stated that the non-gray formulation of the WSGG can be very efficient from a computational point of view, and yields considerably improved predictions, but can lead to significant

discrepancies in high soot loadings. Simplified radiative property models, such as the WSGG or GG models, are often used in computational fluid dynamics (CFD) to simulate combustion problems. The main reason is that implementing more sophisticated models may become extremely time-consuming when fluid flow/combustion/radiative heat transfer are coupled. Examples of works applying those simplified radiative models are presented in Bidi et al. [1], where the authors employed the discrete ordinates method (DOM) to solve the RTE, and the WSGG model to compute non-gray radiation in a cylindrical combustion chamber, with the purpose of studying the radiation effect on the flame structure. Crnomarkovic et al. [4] compared the numerical results obtained when the GG and the WSGG models were applied to model the radiative properties of the gas phase inside a lignite fired furnace. In Yadav et al. [28] the combustion processes of turbulent non-premixed pilot stabilized flames (Sandia Flame D and Delft Flame III) were studied including radiative heat transfer by means of the WSGG model. Guedri et al. [10] investigated the thermal radiation transfer effects on a fire scenario using the narrow band-based WSGG model. In Silva et al. [23], the authors studied the combustion of coal in a commercial thermal power plant with the objective of simulating the operational conditions and identifying factors of inefficiency considering the radiation properties by means of the GG model.

Several researchers have studied new WSGG correlations for application in combustion systems. Taking into account that a limitation of the WSGG is that its correlations coefficients are established for particular ratio of the partial pressures for  $\text{CO}_2$  and  $\text{H}_2\text{O}$  mixtures, Krishnamoorthy [14] obtained parameters for a new WSGG computed from total emissivity correlations encompassing the range of the  $\text{H}_2\text{O}/\text{CO}_2$  ratios encountered within the Sandia Flame D. Predictions from the new model compared favorably against the SLW model and existing benchmarks. With the same motivation, Johansson et al. [12] modified the WSGG to account for various ratios of  $\text{H}_2\text{O}$  and  $\text{CO}_2$  concentrations, covering from oxy-fuel combustion of coal, with dry or wet flue gas recycling, as

well as combustion of natural gas. The modified WSGG model significantly improved the estimation of the radiative source term compared to the gray models, while the accuracy of wall fluxes was similar to the gray models or better.

One important advance in the modeling of radiation in participating gas was the establishment in the past century of high-resolution spectral database that provide spectroscopic parameters to generate the transition lines, such as HITRAN, built at a reference temperature of 296 K for atmospheric applications, and HITEMP, which was established for high temperature applications. Recently, HITEMP2010 [21] was released as a major improvement of previous versions, expanding the number of transition lines for  $\text{H}_2\text{O}$  and  $\text{CO}_2$ , and also allowing for application in temperatures up to 4000 K. Several independent studies have pointed that radiative computations using HITEMP2010 as the most accurate make it the best source of information to date for the development of spectral models for application in high temperature conditions. In recent works, Kangwanpongpan et al. [13] considered the determination and evaluation of new correlations for the WSGG model, fitted from emittance charts calculated from the up-to-date HITEMP 2010 database [21], to predict the radiative transfer in gases under oxy-fuel conditions, while Dorigon et al. [6] generated correlations for typical products of the combustion of methane and fuel oil.

With the objective of evaluating the influence of the different correlations on the radiation and consequently on the overall thermal behavior, this work presents a numerical RANS simulation of turbulent non-premixed combustion of methane–air in a cylindrical chamber taking into account the radiation effect of non-gray gases by means of WSGG model based on two different correlations, the classical ones of Smith et al. [25] and the new ones obtained in Dorigon et al. [6] based on the HITEMP 2010 database. For evaluation of the proposed solution, the case described by Garréton and Simonin [9] was studied, since detailed measurements are available of spatial distributions of major gas species concentrations as well as of the temperature field.

**Fig. 1** Combustion chamber geometry

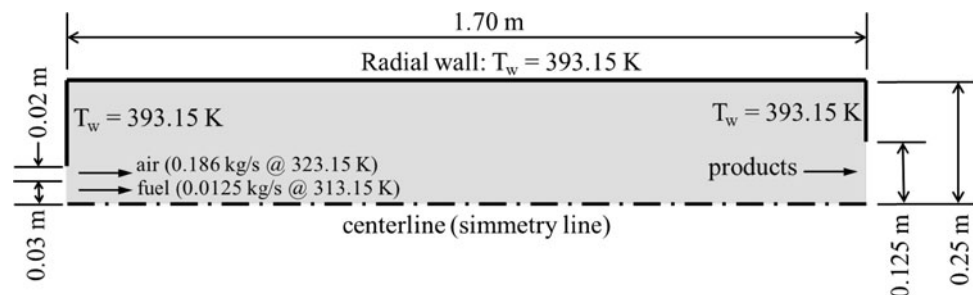


**Table 1** Generic variable, diffusive coefficient, source terms for the conservation equations

Equation	$\phi$	$\Gamma_\phi$	$S^\phi$
Continuity	1	0	0
Axial momentum	$u$	$(\mu + \mu_t)$	$-\frac{\partial p^*}{\partial z} + \frac{\partial}{\partial z}(\mu_t \frac{\partial u}{\partial z}) + \frac{1}{r} \frac{\partial}{\partial r}(r \mu_t \frac{\partial v}{\partial z})$
Radial momentum	$v$	$(\mu + \mu_t)$	$-\frac{\partial p^*}{\partial r} + \frac{\partial}{\partial z}(\mu_t \frac{\partial u}{\partial r}) + \frac{1}{r} \frac{\partial}{\partial r}(r \mu_t \frac{\partial v}{\partial r}) - \frac{(\mu + \mu_t)v}{r^2} + \frac{\rho w^2}{r^2}$
Turbulent kinetic energy	$k$	$(\mu + \frac{\mu_t}{\sigma_k})$	$\left[ \mu_t \left( 2 \left( \frac{\partial u}{\partial z} \right)^2 + \left( \frac{\partial u}{\partial r} + \frac{\partial v}{\partial z} \right)^2 + 2 \left( \frac{\partial v}{\partial r} \right)^2 + 2 \left( \frac{v}{r} \right)^2 \right) \right] - \rho \varepsilon$
Turbulent kinetic energy dissipation	$\varepsilon$	$(\mu + \frac{\mu_t}{\sigma_\varepsilon})$	$C_{1,\varepsilon} \left[ \mu_t \left( 2 \left( \frac{\partial u}{\partial z} \right)^2 + \left( \frac{\partial u}{\partial r} + \frac{\partial v}{\partial z} \right)^2 + 2 \left( \frac{\partial v}{\partial r} \right)^2 + 2 \left( \frac{v}{r} \right)^2 \right) \right] \frac{\varepsilon}{k} - C_{2,\varepsilon} \frac{\varepsilon^2}{k}$
Energy	$h$	$(\frac{\mu}{Pr} + \frac{\mu_t}{Pr_t})$	$S_{rad} + \sum_x \left[ h_x^0 + \int_{T_{ref,x}}^T c_{p,x} dT \right] R_x$
CH <sub>4</sub> , O <sub>2</sub> , CO <sub>2</sub> , CO and H <sub>2</sub> O mass fraction	$y_x$	$(\frac{\mu}{Sc} + \frac{\mu_t}{Sc_t})$	$R_x$

**2 Problem statement**

The physical system chosen to be analyzed in the current investigation consists of the natural gas combustion chamber described in Garréton and Simonin [9], which presents several challenges for radiation modeling in the sense that the flame is turbulent, and with highly non-isothermal, non-homogeneous medium. Several experimental data for temperature and species concentrations profiles along axial and radial coordinates were presented in Garreton and Simonin [9], in addition to the results provided by the investigations of Magel et al. [16], Nieckele et al. [19] and Silva et al. [22], making it a good choice for the current work.

The cylindrical chamber has length and diameter of 1.7 and 0.5 m, respectively, as shown in Fig. 1. Natural gas is injected into the chamber by a duct aligned with the chamber centerline, leading to a non-swirling flame. The burner provides the necessary amount of air and natural gas as required by the process. In all cases, an excess fuel of 5 % (equivalence ratio of 1.05) was prescribed. For a fuel mass flow rate of 0.0125 kg/s at a temperature of 313.15 K, this requires an air mass flow rate of 0.186 kg/s, at a temperature of 323.15 K. The fuel enters the chamber through a cylindrical duct having diameter of 6 cm, while air enters the chamber through a centered annular duct having a spacing of 2 cm. For such mass flow rates, the fuel and air velocities are 7.76 and 36.29 m/s, respectively. The Reynolds number at the entrance, approximately  $1.8 \times 10^4$ , points that the flow is turbulent. The inlet air is composed of oxygen (23 % in mass fraction), nitrogen (76 %) and water vapor (1 %), while the fuel is composed of 90 % of methane and 10 % of nitrogen. The burner power is about 600 kW. The fan and the other external components are not included in the computational domain, although their effects are taken into account through the inlet flow conditions. Buoyancy effects are neglected due

to the high velocities that are provided by the burner. Turbulence intensities of 6 % at the oxidant stream and 10 % at the fuel stream were specified at the inlet. The characteristic length to determine the dissipation at the inlet was specified as 0.04 m at the oxidant opening and 0.03 m at the fuel stream. Both chamber walls, inlet and outlet ducts were modeled as black surfaces.

**3 Mathematical formulation**

The proposed work can be stated as follows: considering a steady turbulent non-premixed methane–air flame in a cylindrical chamber, compute the temperature, chemical species concentrations and velocity fields, and verify the influence of the thermal radiation on the process, taking into account the WSGG model correlations from Smith et al. [25] and Dorigon et al. [6].

**3.1 Governing equations**

Considering the conservation equation for steady incompressible flow in 2D axisymmetric coordinates for the generic variable  $\phi$ , Eq. (1), the mass, momentum in the axial and radial directions,  $k$ – $\varepsilon$  turbulence model, the energy and chemical species conservation equations can be determined by choosing  $\phi$ ,  $\Gamma_\phi$ , and source term  $S^\phi$  from Table 1.

$$\frac{\partial}{\partial z} \left( \rho u \phi - \Gamma_\phi \frac{\partial \phi}{\partial z} \right) + \frac{1}{r} \frac{\partial}{\partial r} \left( r \rho v \phi - r \Gamma_\phi \frac{\partial \phi}{\partial r} \right) = S^\phi \quad (1)$$

In Table 1, the following variables are used:  $z$  and  $r$  are the axial and radial coordinates (both in m),  $u$  and  $v$  are the time average velocities in these respective directions (both in m/s),  $w$  is the average angular velocity (in m/s),  $\rho$  is the density of the gaseous mixture (in kg/m<sup>3</sup>),  $\mu$  is the gaseous mixture dynamic viscosity and  $\mu_t$  is the turbulent viscosity

(both in  $\text{N s/m}^2$ ), defined as  $\mu_t = C_\mu \rho k^2 / \varepsilon$ . The term  $p^* = p - (2/3)k$  is the modified pressure (in Pa),  $C_\mu$  is an empirical constant of the turbulence model ( $C_\mu = 0.09$ ),  $p$  is the combustion chamber operational pressure ( $p = 101,325 \text{ Pa}$  [26]), and  $k$  (in  $\text{m}^2/\text{s}^2$ ) and  $\varepsilon$  (in  $\text{m}^2/\text{s}^3$ ) are the turbulent kinetic energy and its dissipation. Also,  $C_{1,\varepsilon}$  and  $C_{2,\varepsilon}$  are empirical constants of the turbulence model ( $C_{1,\varepsilon} = 1.44$  and  $C_{2,\varepsilon} = 1.92$ ),  $\sigma_k$  and  $\sigma_\varepsilon$  are the Prandtl numbers of the kinetic energy and dissipation, respectively ( $\sigma_k = 1.0$  and  $\sigma_\varepsilon = 1.3$ ).  $Pr_t$  and  $Sc_t$  are the turbulent Prandtl and Schmidt numbers,  $R_\alpha$  [in  $\text{kg}/(\text{m}^3 \text{ s})$ ] is the average volumetric rate of formation or destruction of the  $\alpha$ -th chemical species ( $\text{CH}_4$ ,  $\text{O}_2$ ,  $\text{CO}_2$ ,  $\text{CO}$ ,  $\text{H}_2\text{O}$ ) (this term is briefly discussed in the Sect. 3.2 of this work).  $T$  is the average temperature of the mixture (in K).  $\bar{M}M_\alpha$  (in  $\text{kg}/\text{kmol}$ ),  $c_{p,\alpha}$  [in  $\text{J}/(\text{kg K})$ ],  $h_\alpha^0$  (in  $\text{J}/\text{kg}$ ) and  $T_{\text{ref},\alpha}$  (in K) are the molecular mass, the specific heat, the formation enthalpy and the reference temperature of each  $\alpha$ -th chemical species.  $S_{\text{rad}}$  (in  $\text{W}/\text{m}^3$ ) is the radiative heat source term, calculated as the negative divergence of the radiative heat flux, discussed in the Sect. 3.3 of this work.

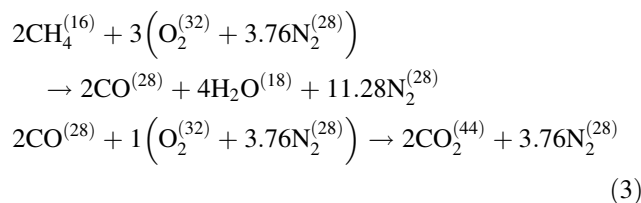
In addition to the conservation laws presented in Table 1, an equation of state is required to calculate the mixture density. Considering the mixture of fuel, oxidant and products as an ideal gas, the equation of state can be written as:

$$\rho = \frac{p}{RT \sum_\alpha y_\alpha / \bar{M}M_\alpha} \quad (2)$$

where  $\bar{R}$  is the universal gas constant [ $\bar{R} = 8.314 \text{ kJ}/(\text{kmol K})$ ], and  $y_\alpha$  (in  $\text{kg}_\alpha/\text{kg}_{\text{tot}}$ ) is the average mass fraction of each  $\alpha$ -th chemical species. Also, it is important to note that in the present work all quantities (as  $u$ ,  $v$ ,  $h$ ,  $T$ ,  $c_p$ ,  $y_\alpha$ ,  $\rho$ ,  $R_\alpha$ ,  $S_{\text{rad}}$ , etc.) are time-averaged (mean), but they are not written with an overbar (usual in RANS simulations) in order to not confuse with molar quantities (which are denoted with an overbar).

### 3.2 Combustion kinetic

As a basic assumption, it is considered that the combustion process occurs at finite rates with methane oxidation taking two global steps according to Eq. (3), given by:



The rate of formation or destruction,  $R_{\alpha,c}$ , of each  $\alpha$ -th species in each  $c$ -th reaction (in this formulation there are two reactions as shown in Eq. (3), so  $c = 2$ ) is obtained by

the Arrhenius–Magnussen’s model [7, 8, 27]), in which the rate of formation or destruction of the chemical species is taken as the smallest one between the values obtained from Arrhenius kinetic rate relation or Magnussen’s equations (Eddy Break-Up) [17]. In Magnussen’s model, the chemical reaction rate is governed by the large-eddy mixing time scale,  $k/\varepsilon$ , and combustion proceeds whenever turbulence is present ( $k/\varepsilon > 0$ ). So, the Arrhenius–Magnussen’s model takes the net reaction rate as the minimum of these two rates, in a manner that the Arrhenius rate act as a kinetic “switch”; once the flame is ignited, the Magnussen’s rate is generally smaller than the Arrhenius rate, and reactions are mixing-limited [8]. The investigation in Silva et al. [22] provided the relative importance to the combustion kinetics in the sense that the authors computed the Damköhler number for the same combustion chamber and found that the combustion process is governed by Arrhenius rates in the flame core and by Magnussen’s rates in all the other regions. This formulation was successfully employed in Nieckele et al. [19] and Silva et al. [22], where all model parameters are described in detail, with the only exception that the activation energy for the first reaction was adjusted here to  $2.3 \times 10^8 \text{ J}/\text{kmol}$ . That adjustment to the activation energy was made to improve the agreement between numerical results and experimental data. However, even with the original activation energy the numerical results were in good agreement with experiments.

The above mentioned two-equation chemistry assumption was employed in the current study for economy of the CPU time. While the two-equation chemistry assumption (and even one-equation) has been used with great success in combustion modeling, it should be recognized that detailed reaction mechanism effects may be very important in several practical applications, especially those involving flame ignition and extinction, or those involving predictions of minor species such as soot, NO and other radicals, which are not the aim of the present work. Also, the chemistry presented in Eq. (3) does not involve soot formation/oxidation, considering that the methane flame is expected to be low sooting. However, it should be recognized that even small quantities of soot can affect the radiation heat transfer, so the inclusion of soot into the analysis would be one possible advance in the research. As for the present study, considering only gas radiation permits assessing the effect of the gas radiation in a turbulent methane flame as well as making a direct comparison of the gas models. The proper understanding of the gas radiation models is an important step prior to investigations including both gaseous species and soot.

The average volumetric rates of formation or destruction of the  $\alpha$ -th chemical species,  $R_\alpha$ , which appears in both the energy and species mass fraction equations, are then

computed from the summation of the volumetric rates of formation or destruction in all the  $c$ -th reactions, where the  $\alpha$ -th species is present, according to:

$$R_\alpha = \sum_c R_{\alpha,c} \tag{4}$$

### 3.3 Radiation modeling

The radiative transfer equation (RTE) for non-scattering media, in cylindrical coordinates, with the discrete ordinates method (DOM), is given by:

$$\frac{\partial I_\eta}{\partial s} = \mu \frac{\partial I_\eta}{\partial r} + \zeta \frac{\partial I_\eta}{\partial z} - \frac{\zeta}{r} \frac{\partial I_\eta}{\partial \phi} = -\kappa_\eta I_\eta + \kappa_\eta I_{b\eta} \tag{5}$$

subjected to boundary conditions for diffusely emitting and reflecting opaque surface:

$$I_{w\eta} = \varepsilon_w I_{bw\eta}(T_w) + \frac{(1 - \varepsilon_w)}{\pi} \int_{\mathbf{n} \cdot \mathbf{s} < 0} I_\eta |\mathbf{n} \cdot \mathbf{s}| d\Omega \tag{6}$$

where  $\mu$ ,  $\zeta$ , and  $\xi$  are the directions,  $\eta$  is the wavenumber,  $I_{b\eta}$  is the blackbody intensity,  $I_\eta$  is the intensity,  $\varepsilon_w$  is wall emissivity,  $\mathbf{n}$  and  $\mathbf{s}$  are the vector normal to the surface element and the vector in the direction of the radiation intensity, respectively,  $\Omega$  is the solid angle,  $T_w$  is wall temperature, and  $\kappa_\eta$  is the spectral absorption coefficient. In the right side of Eq. (5), the first and the second terms represent, respectively, attenuation in the intensity due to absorption and augmentation due to emission. Once the RTE is solved, the radiative heat source, presented in the energy equation as  $S_{rad}$ , is calculated as (where  $\mathbf{q}_r$  is the radiative heat flux):

$$S_{rad} = -\nabla \cdot \mathbf{q}_r = \int_{\Omega} \int_{\eta} (\kappa_\eta I_\eta - \kappa_\eta I_{b\eta}) d\eta d\Omega \tag{7}$$

The spectral absorption coefficient ( $\kappa_\eta$ ) is strongly dependent on the wavenumber, which for participating gases can involve several thousands of spectral lines. Therefore, solving Eq. (5) for all spectral lines is in general excessively time-consuming for coupled solutions of the conservation equations. As such, gas models have been developed to solve the RTE quickly. A brief description of the gas model selected for the present analysis, the WSGG model, is presented in Sect. 3.4.

Considering Reynolds averaging, the mean radiative source term and the mean RTE are unclosed a priori due to instantaneous fluctuating terms related to the absorption coefficient and the blackbody emissive power, a problem known as turbulence–radiation interaction (TRI). According to Coelho [2] and Li and Modest [15], TRI tends to increase the radiation heat transfer, therefore leading to cooler flames. In the current work, these interactions were not accounted for, so all fundamental equations, relations,

results and analysis were related to mean quantities. This is a good assumption for optically thin flames, but should be addressed for in optically thick flames, as implied in Li and Modest [15]. The optical thickness for the flame studied here is about 0.43, which is considered of low-to-medium optical thickness. In this manner, it is expected that this analysis is not pronouncedly affected by neglecting TRI, since the main objective is comparing the radiative calculations using the two different WSGG correlations, while both analyses were taken without this effect.

### 3.4 The weighted-sum-of-gray-gases (WSGG) model

The original formulation of the WSGG model [11] consists of expressing the total gas emittance by weighted-sum-of-gray-gas emittances. The emission weighted factors,  $a_j(T)$ , and the absorption coefficients,  $k_j$ , for the  $j^{\text{th}}$  gray gas were determined from the best fit of the total emissivity with the constraint that the  $a_j$  must sum to the unity. From a more general point of view, the WSGG model can be applied as a non-gray gas model [18], solving the RTE for the  $N_G$  (number of gray gases) plus one ( $j = 0$ , representing spectral windows where  $H_2O$  and  $CO_2$  are transparent to radiation) for a transparent gas:

$$\frac{dI_j}{ds} = -k_j I_j + k_j a_j(T) I_{b,j}(T) \tag{8}$$

with  $j$  varying from 0 to  $N_G$ , and  $I = \sum_0^{N_G} I_j$ . The functional dependence of the emission weighted factors with temperature is generally fitted by polynomials, where the polynomial coefficients ( $b_j$ ) as well as the absorption coefficients for each gray gas can be tabulated. For  $CO_2/H_2O$  mixtures, these coefficients are generally established for particular ratios of the partial pressure,  $p_{H_2O}/p_{CO_2}$ , which could limit the application of the model. In the present study, the emission weighted factors polynomial coefficients and the absorption coefficients were taken from both formulations of Dorigon et al. [6] and Smith et al. [25] for  $p_{H_2O}/p_{CO_2} = 2$ . Dorigon et al. [6] obtained WSGG model coefficients fitted from HITEMP2010 molecular spectroscopic experimental database [21], which is the latest molecular spectroscopic database that is available nowadays for high temperatures. In the same study, Dorigon et al. [6] compared the results obtained with the new coefficients against LBL benchmark calculations for one-dimensional non-isothermal non-homogeneous problems, finding consistently satisfactory agreement with maximum and average errors of about 5 and 2 % for different test cases. Table 2 shows the coefficients proposed in Dorigon et al. [6], while Table 3 presents the classical coefficients of Smith et al. [25]. It is assumed here that the contribution from other radiating species, such as CO and  $CH_4$ , is negligible. The contribution from CO in the

**Table 2** WSGG model coefficients [6]

$j$	$k_{p,j}$ ( $\text{m}^{-1} \text{atm}^{-1}$ )	$b_{j1} \times 10^1$	$b_{j2} \times 10^4$ ( $\text{K}^{-1}$ )	$b_{j3} \times 10^7$ ( $\text{K}^{-2}$ )	$b_{j4} \times 10^{10}$ ( $\text{K}^{-3}$ )	$b_{j5} \times 10^{14}$ ( $\text{K}^{-4}$ )
1	0.192	0.5617	7.8440	-8.5630	4.2460	-7.4400
2	1.719	1.4260	1.7950	-0.1077	-0.6972	1.7740
3	11.370	1.3620	2.5740	-3.7110	1.5750	-2.2670
4	111.016	1.2220	-0.2327	-0.7492	0.4275	-0.6608

$p_{\text{H}_2\text{O}}/p_{\text{CO}_2} = 2$

**Table 3** WSGG model coefficients [25]

$j$	$k_{p,j}$ ( $\text{m}^{-1} \text{atm}^{-1}$ )	$b_{j1} \times 10^1$	$b_{j2} \times 10^4$ ( $\text{K}^{-1}$ )	$b_{j3} \times 10^7$ ( $\text{K}^{-2}$ )	$b_{j4} \times 10^{11}$ ( $\text{K}^{-3}$ )
1	0.4201	6.508	-5.551	3.029	-5.353
2	6.516	-0.2504	6.112	-3.882	6.528
3	131.9	2.718	-3.118	1.221	-1.612

$p_{\text{H}_2\text{O}}/p_{\text{CO}_2} = 2$

combustion gases is negligible, as long as its concentration does not exceed relatively high values of the order of 0.05 %, while the contribution from CH<sub>4</sub> is even lower [3].

### 4 Results and discussions

Figure 1 depicts the thermal boundary conditions of the cylindrical chamber: symmetry in the centerline, and prescribed temperature on the wall, equal to 393.15 K. The set of equations were solved using the finite volume method [20] by means of a Fortran code. The power law was applied as the diffusive–advective interpolation function on the faces of the control volumes. The pressure–velocity coupling was made by the SIMPLE method. The resulting system of algebraic equations was solved by the TDMA algorithm, with block correction in all equations except for the  $k$  and  $\epsilon$  equations. A grid with 50 volumes in the radial direction and 90 volumes in the axial direction was used. The numerical accuracy was checked by comparing the predicted results calculated using the above grid with those obtained using coarser and thinner grids. Table 4 provides the radiant fraction (defined as the ratio between the integral of  $S_{\text{rad}}$  over the computational domain and the heat

released in the combustion reaction) as well as the convective and radiative heat transfer rates on the combustion chamber radial wall obtained with different grids, together with the relative deviation for each value in relation to the value of the grid immediately coarser. Results in Table 4 were obtained using coefficients of Smith et al. [25] WSGG model for radiation calculations. The radiative transfer calculations were performed using the same spatial grids, and S<sub>6</sub> quadrature. As found, the 50 × 90 grid provided grid independent results, and required reasonable computational effort, and was applied in all test cases presented in this study. The 50 × 90 grid, illustrated in Fig. 2, is non-uniformly spaced in the radial direction but uniformly spaced in the axial direction. Convergence criteria were based on the imposition that the normalized residual mass in the SIMPLE method is 10<sup>-8</sup>. For the other equations the maximum relative variation between iterations is 10<sup>-6</sup>. The radiative transfer in molecular gases depends on the number of (radiative) participant molecules per unit volume. In the present work, the pressure absorption coefficient for the  $j$ -th gray gas for the WSGG model,  $k_{p,j}$  (in  $\text{m}^{-1}\text{atm}^{-1}$ ), present in Tables 2 and 3, was multiplied by the summation of the partial pressures of H<sub>2</sub>O and of CO<sub>2</sub> for each computational volume cell, obtaining the absorption coefficient for the  $j$ -th gray gas,  $k_j$  (in  $\text{m}^{-1}$ ), necessary to compute Eq. (8). In this manner, inhomogeneity of H<sub>2</sub>O and CO<sub>2</sub> concentrations inside the chamber were also taken into account to compute the radiative transfer.

In order to study the effect of the radiative transfer and radiative properties modeling on the thermal behavior, three different scenarios were considered. In the first scenario, radiation was completely ignored to analyze the

**Table 4** Radiant fraction and convective and radiative heat transfer rates on the combustion chamber radial wall obtained with different grids

Grid	$f_{\text{rad}}$ (%)	% Dev.	Heat transfer rate on the combustion chamber radial wall			
			Convection (kW)	% Dev.	Radiation (kW)	% Dev.
35 × 70	12.219	–	71.119	–	62.765	–
40 × 80	12.150	0.565	71.551	0.607	62.145	0.988
45 × 85	12.124	0.214	71.822	0.379	61.889	0.412
50 × 90	12.113	0.091	72.012	0.265	61.768	0.195
55 × 110	12.106	0.058	72.063	0.071	61.727	0.066

**Fig. 2** Grid with  $50 \times 90$  volumes that was employed in the calculations

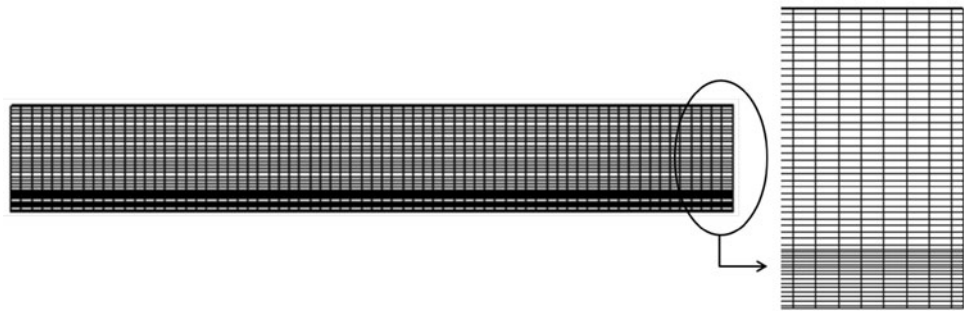
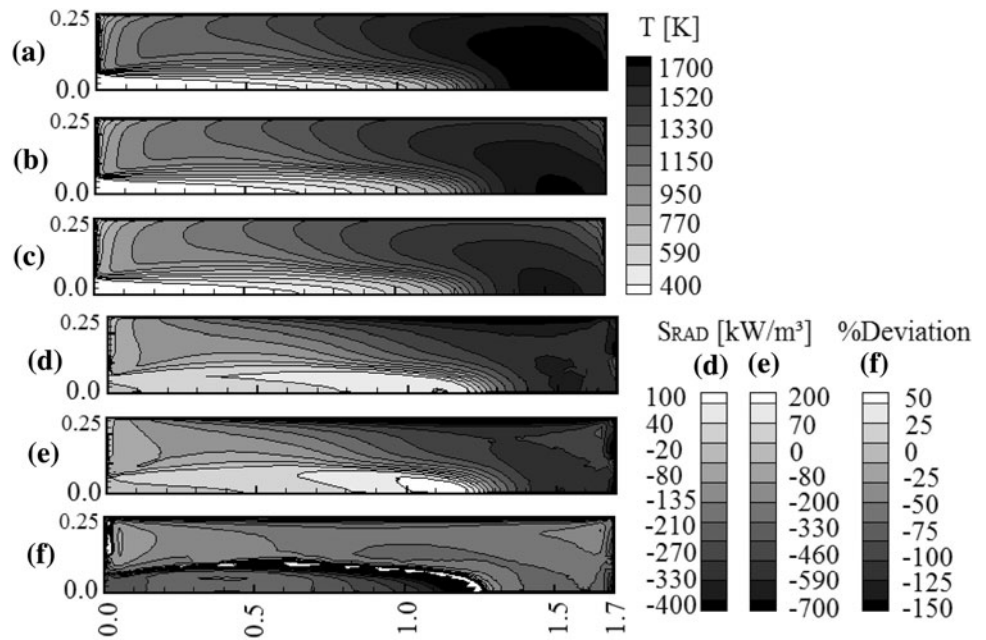


**Fig. 3** Temperature fields for the three scenarios: **a** radiation neglected; **b** radiation computed with Smith et al. [25] correlations; **c** radiation computed with Dorigon et al. [6] correlations. Radiative heat source computed with: **d** Smith et al. [25] correlations; **e** Dorigon et al. [6] correlations; **f** relative deviation between **d** and **e**



importance of radiation in this particular flame simulation. In the second and third scenarios, radiation was considered and the absorption coefficient was modeled using two different WSGG models. Comparisons were made to verify how the radiative scenarios affect the temperature,  $H_2O$  concentration,  $CO_2$  concentration, and radiative heat source fields, as well as some of the thermal quantities, such as the radiant fraction and heat fluxes through chamber walls.

Figure 3 shows the results of the temperature and the radiative heat source. Figure 3a–c shows the temperature plots obtained for the three scenarios that were described above. Figure 3d–f shows the radiative heat source obtained for the second and third radiative scenarios, as well as the relative deviation between them, computed as:

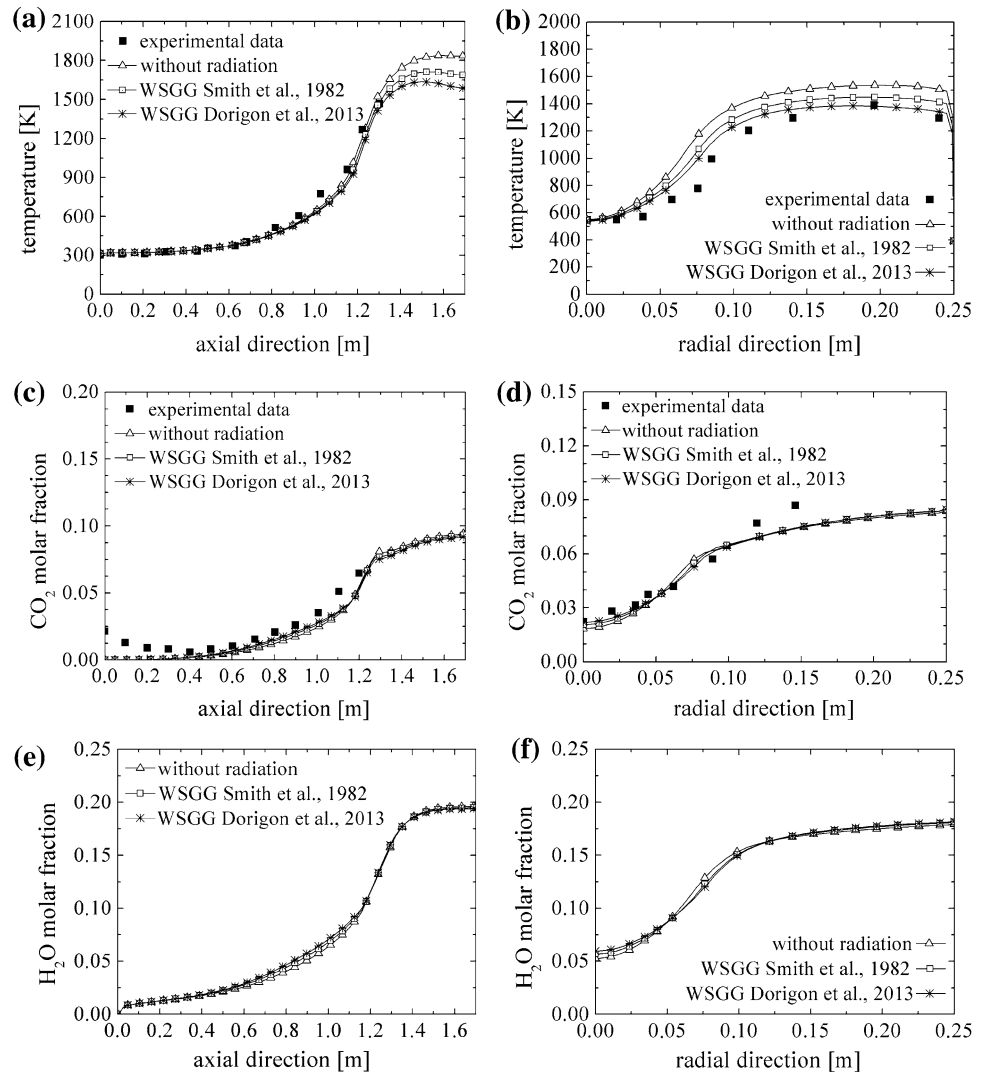
$$\%Deviation = 100 \frac{S_{rad,Smith} - S_{rad,Dorigon}}{S_{rad,Smith}} \quad (9)$$

In Eq. (9) subscripts Smith and Dorigon indicate which WSGG model correlations were used in the calculation of

$S_{rad}$ . As can be seen in Fig. 3a–c, consideration of the different WSGG models plays an important role in the temperature field. Flame peak temperatures were 1,839, 1,714, and 1,636 K, for scenarios neglecting radiation, and considering radiation with Smith et al. [25] and with Dorigon et al. [6] WSGG correlations, respectively. While these peaks are local, they can be taken as a measure to characterize the entire temperature field. Neglecting radiation, the maximum temperature in the medium was 125 and 203 K higher than the maximum temperatures that were obtained for the cases with radiation using the correlations of Smith et al. [25] and with Dorigon et al. [6], respectively.

As with the temperature field, radiation fields also changed significantly as a result of the different WSGG model correlations. Figure 3d, e shows the radiative heat source contours. In the regions with the highest temperatures, emission of radiation exceeds absorption, leading to negative radiative heat sources. On the other hand, absorption exceeds emission in the regions with the lowest

**Fig. 4** Axial profiles of **a** temperature, **c** H<sub>2</sub>O and **e** CO<sub>2</sub> along the chamber centerline, and radial profiles of **b** temperature, **d** H<sub>2</sub>O and **f** CO<sub>2</sub> at  $z = 0.912$  m



temperatures, leading to positive radiative heat sources. Also, Fig. 3f shows the relative deviation of the radiative heat source obtained from different WSGG model correlations, computed per Eq. (9). The radiative heat source calculated with Dorigon et al. [6] correlations is higher than the one calculated with Smith et al. [25]. The higher differences are located at the flame core, with relatively low temperature levels and positive net radiative source (absorbing region).

Figure 4 shows the temperature, H<sub>2</sub>O molar fraction and CO<sub>2</sub> molar fraction profiles along the chamber centerline and along the radial direction at axial position 0.912 m from the chamber entrance, considering the three scenarios described above in addition to experimental data from Garréton and Simonin [9] (data not available for H<sub>2</sub>O). It is observed that the temperature values and temperature gradients are decreased when radiation heat transfer is considered since there is an additional heat transfer mode inside the computational domain. The same behavior is

observed comparing the results obtained with the different WSGG model correlations, i.e., since the use of Dorigon et al. [6] correlations provides higher radiative heat source than Smith et al. [25] correlations, the temperature and gradient levels are smaller for the former correlations. The same analysis can be implied from Fig. 3. Since the reaction rate coefficients depend on the temperature, radiation should be expected to affect the formation and destruction of the species involved in the process. In spite of this, the mean variations of H<sub>2</sub>O and CO<sub>2</sub> molar fractions using the different correlations are less than 1.0 %, showing that the species molar fractions were considerably less affected by the radiative modeling than the temperature. This could be caused by the use of the reduced-chemistry assumption, in which chemical reaction rate is primarily controlled by turbulent mixing and, therefore, is less sensitive to temperature. On the other hand, the heat transfer rate through chamber side wall, the net radiative heat loss and the radiant fraction strongly depended on the radiation

**Fig. 5** Axial profiles of the radiative heat source along the chamber centerline

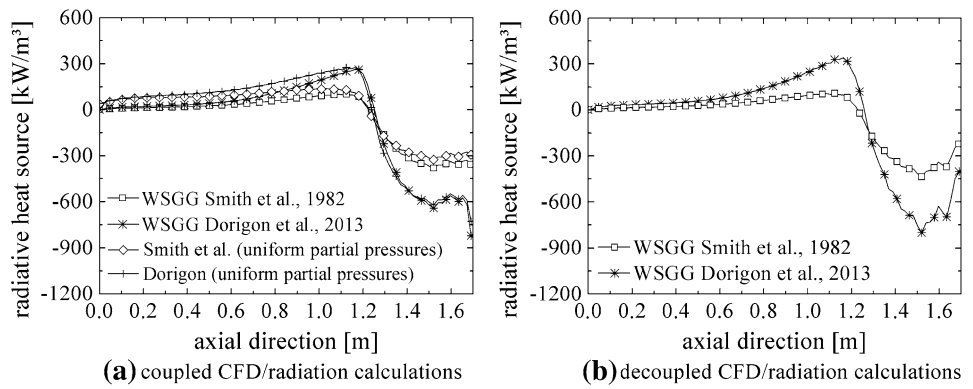


**Table 5** Average relative deviation expressing the difference between experimental data and numerical results for both scenarios without radiation and with radiation

	Without radiation	With radiation <sup>a</sup>	With radiation <sup>b</sup>
Figure 4a (%)	2.0	2.2	2.6
Figure 4b (%)	13.4	8.5	5.5
Figure 4c (%)	11.2	9.6	9.0
Figure 4d (%)	6.9	5.8	5.1

<sup>a</sup> Using WSGG correlations of Smith et al. [25]

<sup>b</sup> Using WSGG correlations of Dorigon et al. [6]

modeling, as revealed in Figs. 3, 5, and Tables 6, 7. Also, Fig. 4 shows that for all the radiation models the mean temperature and the mean molar fraction of CO<sub>2</sub> follow the experimental data trend, despite some deviations, which had probably minor relation to the choice of the radiation modeling, arising from limitations of the other models (turbulence and combustion).

Table 5 presents the average relative deviation computed as  $\%Dev = \sum_{i=1}^n \frac{1}{n} [100(V_{exp,i} - V_{rad,i})/V_{exp,max}]$  expressing the difference between experimental data ( $V_{exp}$ ) and numerical results ( $V_{rad}$ ) for both scenarios without radiation and with radiation calculated with Smith et al. [25] and Dorigon et al. [6] correlations for all the results of Fig. 4. These deviations indicate that the major effect of radiation is on the temperature field, especially in the radial direction profiles, with minor effect on CO<sub>2</sub> molar fractions, which corroborates the results shown in Fig. 4.

An additional view of the effect of thermal radiation is presented in Table 6, which shows the heat transfer rate through the chamber wall. The inclusion of thermal radiation has a major effect in the radiation–convection combined heat transfer mode, leading to an increase in the total heat transfer from 79.73 kW (only convection, without radiation transfer) to a maximum of 160.09 kW (sum of convection and radiation transfer). The pattern of these results agrees with Silva et al. [22], where it was shown

that the predicted heat transfer through the chamber wall was approximately doubled when radiation was taken into account. It is interesting to note that when thermal radiation is included, the convective transfer decreases in comparison to when thermal radiation is neglected, since the temperature gradients in the chamber are reduced due to the additional volumetric heat source. Also, the results show that radiation transfer is increased when the new WSGG model correlations are used, as expected, since the radiative heat source (Fig. 3) is higher using them.

The role of using different WSGG correlations on radiative heat transfer can be alternatively shown by isolating their effects on the radiation calculations alone. This can be done by freezing the species molar fraction and temperature fields, and then calculating radiation fields using WSGG model correlations from Smith et al. [25] and Dorigon et al. [6]. These calculations are decoupled from the other mechanisms, and, therefore, uncertainties arising from turbulence and combustion models do not influence the comparison. This procedure was applied using the same converged temperature, and H<sub>2</sub>O and CO<sub>2</sub> fields obtained from the simulation which neglects radiation heat transfer. The results of this analysis are presented as “decoupled CFD/radiation calculations” in Table 7 and Fig. 5. It is emphasized that all the other radiation results presented previously or further on the present work were obtained with coupled calculations.

An important quantity that describes the overall radiation field of a flame is the net radiative heat loss from the flame and its normalized variable, the radiant fraction ( $f_{rad}$ ). The net radiative heat loss corresponds to the integral of  $S_{rad}$  over the computational domain; the radiant fraction is the ratio of this value to the heat released in the combustion reaction. These quantities were calculated and are shown in Table 7. The radiation loss and the corresponding radiant fraction from the present flame have significant values. The radiant fraction increased considerably using the WSGG model correlations proposed by Dorigon et al. [6]. Also, the radiant fraction follows the same trend for both coupled and decoupled CFD/radiation calculations, i.e., it increases

**Table 6** Heat transfer rate on the combustion chamber radial wall

	Without radiation	With radiation <sup>a</sup>	With radiation <sup>b</sup>
Convection heat transfer rate (kW)	79.73	72.01	62.61
Radiative heat transfer rate (kW)	0.00	61.77	97.48
Total rate (radiation + convection) (kW)	79.73	133.78	160.09

<sup>a</sup> Using WSGG correlations of Smith et al. [25]

<sup>b</sup> Using WSGG correlations of Dorigon et al. [6]

**Table 7** Predicted net radiative heat loss and radiant fraction

	Coupled CFD/radiation calculations		Decoupled CFD/radiation calculations	
	Net radiative heat loss (kW)	$f_{rad}$ (%)	Net radiative heat loss (kW)	$f_{rad}$ (%)
WSGG [25]	71.12	12.11	85.68	14.49
WSGG [6]	115.18	19.73	166.31	28.12

due to the different WSGG model correlations. In addition, the net radiative heat loss and radiant fraction from “decoupled calculations” are higher than from “coupled calculations” since the temperatures are higher for calculations without radiation. Using this temperature field to compute the radiation heat transfer will lead to higher values. The overall energy balance on the combustion chamber, as well as the radiative energy balance, was verified during all computations. The differences between the radiative heat transfer rates reported on Table 6 and the net radiative heat losses reported on Table 7 are because results on Table 6 are related only to rates on the cylindrical wall of the chamber, not taking into account the annular walls located at the entrance and exit of the chamber, as well as the inlet and outlet boundaries of the chamber.

Figure 5 presents profiles of the radiative heat source along the axial direction at the chamber centerline for coupled and decoupled CFD/radiation calculations cases. As seen, the radiative heat source is essentially the same in both coupled and decoupled cases, with a multiplication factor between them in some regions that supports the results of Table 7. In addition, Fig. 5a also shows an important and interesting result, identified as “Smith et al./Dorigon et al. (uniform partial pressures)”. In those computations, the radiative heat source was computed disregarding the effect to inhomogeneity of H<sub>2</sub>O and CO<sub>2</sub> concentrations inside the combustion chamber, i.e., the pressure absorption coefficient for the *j*-th gray gas for the WSGG model,  $k_{p,j}$  (in m<sup>-1</sup>atm<sup>-1</sup>), present in Tables 2 and

3, was not multiplied by the summation of the partial pressures of H<sub>2</sub>O and of CO<sub>2</sub> for each computational volume cell to obtain the absorption coefficient for the *j*-th gray gas,  $k_j$  (in m<sup>-1</sup>), but, in that case,  $k_{p,j}$  was multiplied by the summation of constant values of partial pressures of H<sub>2</sub>O and of CO<sub>2</sub> ( $p_{H_2O} = 0.2$  atm and  $p_{CO_2} = 0.1$  atm). This result allowed verifying the effect of inhomogeneity of H<sub>2</sub>O and CO<sub>2</sub> concentrations inside the combustion chamber on the radiative heat transfer. Despite the difference shown in Fig. 5a not being large, its effect is not negligible. For example, disregarding the inhomogeneity of H<sub>2</sub>O and CO<sub>2</sub> concentrations leads to an increase on computed flame peak temperature from 1,714 to 1,722 K, and to a reduction on the radiant fraction from 12.11 to 10.95 %, when using classical WSGG correlations. The variations are from 1,636 to 1,645 K and from 19.73 to 18.42 % when using Dorigon et al. [6] WSGG correlations.

## 5 Conclusions

RANS simulations of a turbulent non-premixed methane–air flame in a cylindrical chamber were performed to investigate the radiation effects of non-gray gases by means of two different WSGG models: the well-known correlations of Smith et al. [25] and the recently obtained correlations of Dorigon et al. [6] based on the up-to-date HITEMP2010. A two-step global reaction mechanism was used and turbulence modeling was considered via standard *k*– $\epsilon$  model. The discrete ordinate method was employed to solve the radiative transfer equation. This work showed the importance of accurate predictions for the radiative heat transfer for combustion problems. The comparison of the results obtained with the two WSGG correlations showed that temperature, radiative heat source, heat transfer through chamber wall and radiant fraction were sensible and affected by the different WSGG model correlations, while its effect on species concentrations was of minor relevance. Since the radiative heat source changed significantly with the two correlations, it is conclusive that, to achieve an accurate prediction of the temperature field and wall chamber heat transfer, it is mandatory to use an accurate radiation model in the simulations. Also, the numerical results obtained for the case considering the new WSGG model correlations were closer to the experimental data [9] than the case with the classical correlations. It was also investigated the effects of inhomogeneities in the concentrations of H<sub>2</sub>O and CO<sub>2</sub> inside the combustion chamber on the radiative heat transfer, which proved to be of moderate importance in this particular application. Overall, this study shows that radiation heat transfer and radiative properties modeling are very important issues in combustion predictions. Some possible future advances in

the radiation analysis include kinetics for soot formation, a needed step prior to modeling combined soot and gas radiation, and considering turbulence–radiation interaction (TRI).

**Acknowledgments** Authors FHRF and HAV thank CNPq (Brazil) for research Grants 304728/2010-1, 473899/2011-6 and 470325/2011-9, 303823/2012-7, respectively.

## References

- Bidi M, Hosseini R, Nobari MRH (2008) Numerical analysis of methane–air combustion considering radiation effect. *Energy Convers Manage* 49:3634–3647
- Coelho PJ (2007) Numerical simulation of the interaction between turbulence and radiation in reactive flows. *Prog Energy Combust Sci* 33:311–383
- Coelho PJ, Teerling OJ, Roekaerts D (2003) Spectral radiative effects and turbulence/radiation interaction in a non-luminous turbulent jet diffusion flame. *Combust Flame* 133:75–91
- Crnomarkovic N, Sijercic M, Belosevic S, Tucakovic D, Zivanovic T (2013) Numerical investigation of processes in the lignite-fired furnace when simple gray gas and weighted sum of gray gases models are used. *IJHMT* 56:197–205
- Demarco R, Consalvi JL, Fuentes A, Melis S (2011) Assessment of radiative property models in non-gray sooting media. *Int J Therm Sci* 50:1672–1684
- Dorigon LJ, Duciak G, Brittes R, Cassol F, Galarça M, França FHR (2013) WSGG correlations based on HITEMP 2010 for computation of thermal radiation in non-isothermal, non-homogeneous H<sub>2</sub>O/CO<sub>2</sub> mixtures. *IJHMT* 64:863–873
- Eaton AM, Smoot LD, Hill SC, Eatough CN (1999) Components, formulations, solutions, evaluations and applications of comprehensive combustion models. *Prog Energy Combust Sci* 25:387–436
- (2009) In: Fluent (ed) *Fluent Theory Guide*. Fluent Incorporated, New Hampshire
- Garréton D, Simonin O (1994) “Final results”, *Proceedings of the First Workshop of Aerodynamics of Steady State Combustion Chambers and Furnaces*, EDF-ERCOFTAC, vol 25, pp 29–35
- Guedri K, Borjini MN, Jeguirim M, Brilhac J, Saïd R (2011) Numerical study of radiative heat transfer effects on a complex configuration of rack storage fire. *Energy* 36:2984–2996
- Hottel HC, Sarofim AF (1967) *Radiative Transfer*. McGraw-Hill Book Company, New York
- Johansson R, Leckner B, Andersson K, Johnsson F (2011) Account for variations in the H<sub>2</sub>O to CO<sub>2</sub> molar ratio when modeling gaseous radiative heat transfer with the weighted-sum-of-grey-gases model. *Combust Flame* 158:893–901
- Kangwanpongpan T, França FHR, Silva RC, Schneider PS, Krautz HJ (2012) New correlations for the weighted-sum-of-gray-gases model in oxy-fuel conditions based on HITEMP 2010 database. *IJHMT* 55:7419–7433
- Krishnamoorthy G (2010) A new weighted-sum-of-gray-gases model for CO<sub>2</sub>–H<sub>2</sub>O gas mixtures. *Int Comm Heat Mass Transf* 37:1182–1186
- Li G, Modest MF (2002) Importance of turbulence–radiation interactions in turbulent reacting flows, *Proceedings of the 2002 ASME International Mechanical Engineering Congress and Exhibition*, New Orleans, Louisiana, USA
- Magel HC, Schnell U, Hein KRG (1996) Modeling of hydrocarbon and nitrogen chemistry in turbulent combustor flows using detailed reaction mechanisms, *Proceedings of the 3rd Workshop on Modeling of Chemical Reaction Systems*, Heidelberg
- Magnussen BF, Hjertager BH (1977) On mathematical models of turbulent combustion with special emphasis on soot formation and combustion, *Proceedings of the 16th Symposium (International) on Combustion*, The Combustion Institute, Cambridge, MA, USA, pp 719–729
- Modest MF (1991) The weighted-sum-of-gray-gases model for arbitrary solution methods in radiative transfer. *ASME J Heat Transf* 113:650–656
- Nieckele AO, Naccache MF, Gomes MSP, Carneiro JE, Serfaty R (2001) Models evaluations of combustion process in a cylindrical furnace, *Proceedings of 2001 ASME International Mechanical Engineering Congress and Exposition*, New York, NY, USA
- Patankar SV (1980) *Numerical heat transfer and fluid flow*. Hemisphere, Washington, DC
- Rothman LS, Gordon IE, Barber RJ, Dothe H, Gamache RR, Goldman A, Perevalov VI, Tashkun SA, Tennyson J (2010) HITEMP, the high-temperature molecular spectroscopic database. *JQS & RT* 111:2130–2150
- Silva CV, França FHR, Vielmo HA (2007) Analysis of the turbulent, non-premixed combustion of natural gas in a cylindrical chamber with and without thermal radiation. *Combust Sci Tech* 179:1605–1630
- Silva CV, Indrusiak MLS, Beskow AB (2010) CFD analysis of the pulverized coal combustion processes in a 160 MWe tangentially-fired-boiler of a thermal power plant. *JBSMSE* 32:427–436
- Smith TF, Al-Turki AM, Byun KH, Kim TK (1987) Radiative and conductive transfer for a gas/soot mixture between diffuse parallel plates. *J Thermophys Heat Transf* 1:50–55
- Smith TF, Shen ZF, Friedman JN (1982) Evaluation of coefficients for the weighted sum of gray gases model. *J Heat Transf* 104:602–608
- Spalding DB (1979) *Combustion and mass transfer*. Pergamon Press, Inc., New York
- Turns SR (2000) *An introduction to combustion: concepts and applications*, McGraw-Hill, New York
- Yadav R, Kushari A, Eswaran V, Verma AK (2013) A numerical investigation of the Eulerian PDF transport approach for modeling of turbulent non-premixed pilot stabilized flames. *Combust Flame* 160:618–634